Activating Electroluminescence of Charged Naphthalene Diimide Complexes Directly Adsorbed on a Metal Substrate

Vibhuti Rai[1,*] Lukas Gerhard,[1] Nico Balzer,[2] Michal Valášek,[2] Christof Holzer,[3] Liang Yang,[2,4] Martin Wegener,[2,4] Carsten Rockstuhl,[2,3] Marcel Mayor,[2,5,6] and Wulf Wulfhekel[1,7]

[1]*Institute for Quantum Materials and Technologies, Karlsruhe Institute of Technology (KIT), D-76344 Eggenstein-Leopoldshafen, Germany*
[2]*Institute of Nanotechnology, Karlsruhe Institute of Technology (KIT), D-76344 Eggenstein-Leopoldshafen, Germany*
[3]*Institute of Theoretical Solid State Physics, Karlsruhe Institute of Technology (KIT), D-76128 Karlsruhe, Germany*
[4]*Institute of Applied Physics, Karlsruhe Institute of Technology (KIT), D-76128 Karlsruhe, Germany*
[5]*Department of Chemistry, University of Basel, St. Johannsring 19, CH-4056 Basel, Switzerland*
[6]*Lehn Institute of Functional Materials (LIFM), Sun Yat-Sen University (SYSU), Xingang West Road, Guangzhou, China*
[7]*Physikalisches Institut, Karlsruhe Institute of Technology (KIT), D-76128 Karlsruhe, Germany*

Electroluminescence from single molecules adsorbed on a conducting surface imposes conflicting demands for the molecule-electrode coupling. To conduct electrons, the molecular orbitals need to be hybridized with the electrodes. To emit light, they need to be decoupled from the electrodes to prevent fluorescence quenching. Here, we show that fully quenched 2,6-core-substituted naphthalene diimide derivative in a self-assembled monolayer directly deposited on a Au(111) surface can be activated with the tip of a scanning tunneling microscope to decouple the relevant frontier orbitals from the metallic substrate. In this way, individual molecules can be driven from a strongly hybridized state with quenched luminescence to a light-emitting state. The emission performance compares in terms of quantum efficiency, stability, and reproducibility to that of single molecules deposited on thin insulating layers. Quantum chemical calculations suggest that the emitted light originates from the singly charged cationic pair of the molecules.

The potential of functional molecules is unlocked when they combine the characteristics of conventional device functionalities with properties inherent to individual nano-objects, such as photon emission characteristics, self-assembly, or switching. The successful integration of individual molecules as functional units for potential applications requires controlled manipulation via external stimuli. Scanning tunneling microscopy (STM) has been proven to be a capable technique to study and manipulate single molecules immobilized on surfaces [1–7]. In combination with a photon collection setup, its functionality can be extended to detect the light emitted from the junction [8–16]. For a molecule to emit light in a STM junction, it needs to be decoupled from the metallic substrate in order to reduce the hybridization of molecular orbitals. This is typically achieved by inserting a thin insulating layer of NaCl [10,14,15,17–25]. A promising alternative is the functionalization of the light-emitting chromophore with a suitable spacer group [26,27] that preferentially binds to the metal and decouples the chromophore. Reported light emission from such systems is, however, less reproducible due to the complex nature of the molecules [28–33]. In both approaches, the decoupling of a given molecule is fixed.

In this Letter, we report our finding that it is possible to activate the electroluminescence (EL) of 2,6-core-substituted

naphthalene diimide molecules (Tpd-sNDI) adsorbed directly on a metal surface by electronically decoupling them from the underlying substrate with the help of a STM tip. We observe that in order to emit light, both orbitals involved in the optical transition need to be electronically decoupled.

Figure 1(a) shows the chemical structure of the Tpd-sNDI molecule consisting of a triphenylmethane platform with three acetyl-protected thiol anchors with a 2,4,6-trimethylphenylsulfanyl core-substituted NDI chromophore linked via an alkyne spacer. Synthesis and spray deposition of the solution onto a clean Au(111) surface have been discussed in our recent work [26,33] (also see Materials and Methods in the Supplemental Material [34]). After postannealing to about 180 °C, the molecules adsorb flat on the surface and form extended ordered islands with domains that are aligned along the $\langle 1\bar{1}0 \rangle$ axes of the Au(111) surface [see Fig. 1(b)]. Figure 1(c) shows a close-up view of the molecular island. Superimposing the molecular structure indicates that the molecules arrange in a configuration with the long axis [red arrow in Fig. 1(a)] of the molecule parallel to the $\langle 1\bar{1}0 \rangle$ axes of the Au(111) surface and grouped in pairs of opposite orientation [see Fig. 1(d)] [33]. This way, the molecules form a commensurable lattice with a monoclinic unit cell with unit vectors
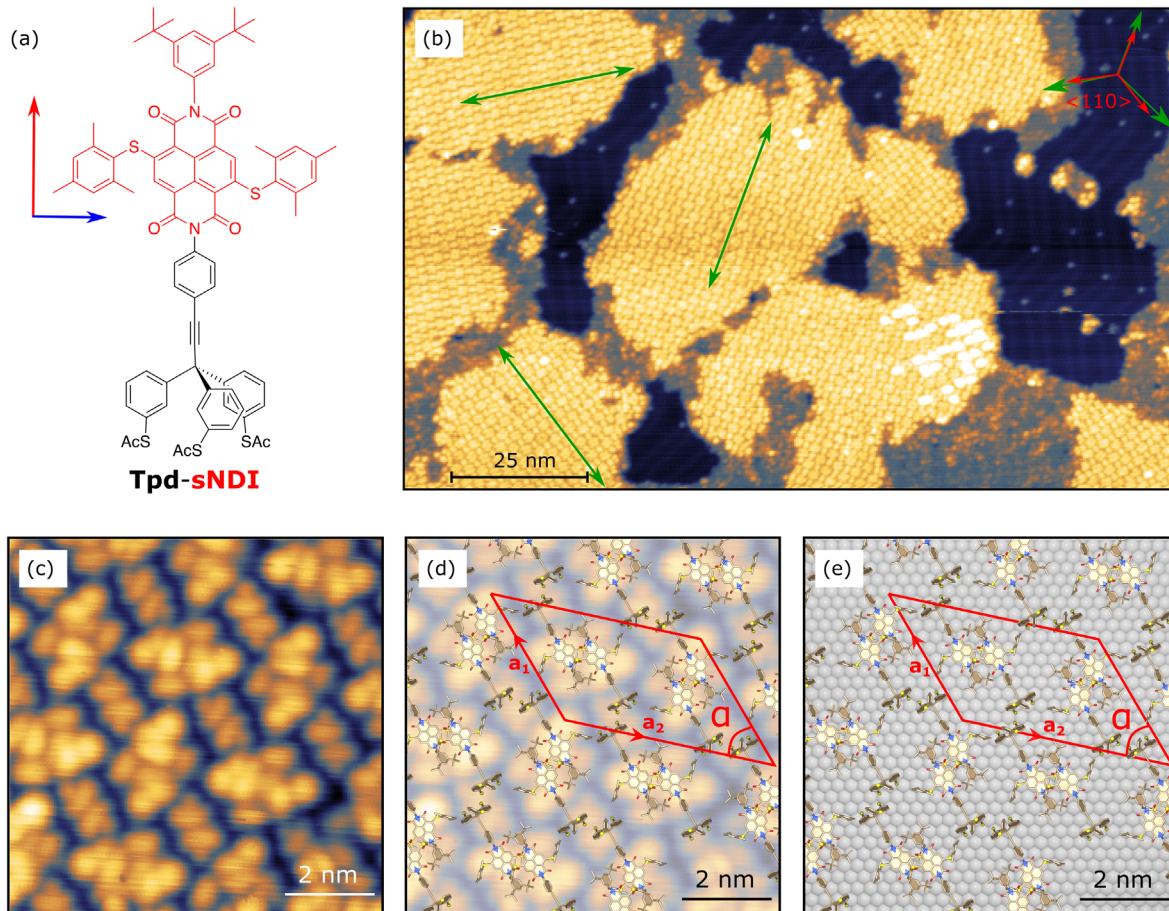
FIG. 1.   Adsorption configuration of Tpd-sNDI molecules on Au(111). (a) Chemical structure of Tpd-sNDI as synthesized, comprising a chromophore (red) and a tripodal anchor (black). Long and short axis of the molecule are represented by red and blue arrows, respectively. (b) STM image of ordered domains of Tpd-sNDI molecules ($U = 1.8$ V, $I = 2$ pA). Green arrows show the orientation of the molecular islands, red arrows show the $\langle 1\bar{1}0 \rangle$ directions of Au(111). (c) Enlarged STM image ($U = -2.5$ V, $I = 12$ pA) of a molecular island. (d) Molecular structure superimposed to scale on (c). A monoclinic unit cell (3.24 nm × 4.79 nm = 11.44 nm², $\alpha = 47.5^0$) of the island is represented in red containing four molecules. (e) Atomic lattice of the Au(111) surface with the suggested molecular arrangement superimposed to scale.

$a_1 = \begin{pmatrix} 0 \\ 11 \end{pmatrix}$ and $a_2 = \begin{pmatrix} 14 \\ 4 \end{pmatrix}$ (3.24 × 4.79 nm², $\alpha = 47.5°$) comprising four molecules. In this model, two sulfur atoms of each molecule's foot structure and the entire chromophore adsorb on identical positions with respect to the top atomic layer [see Fig. 1(e)].

Originally, the molecular complexes were designed to stand upright on the tripodal anchor, decoupling the sNDI chromophore from the substrate, which failed because of the dimensional mismatch of the molecular subunits. Evidently, the van der Waals interaction between the large molecule and the substrate overcomes the binding energy of the thiol groups of the feet. As a consequence of the flat adsorption configuration with the sNDI group in contact with the substrate, EL of the molecules is quenched. However, this configuration allows manipulation with the STM tip. By applying high positive sample bias voltages ($U \geq 2.5$ V), the apparent height can be increased by ~160 pm.

Comparing the topographies before [see Fig. 2(a)] and after [Fig. 2(b)] the switching clearly shows that the difference [see Fig. 2(c)] is restricted to the chromophore part, while the part related to the foot structure remains unchanged. This small change in the apparent height of the chromophore part of the molecule alone does not agree with a reorientation of the molecules to the upright configuration with the long axis perpendicular to the surface. Instead, we speculate that the lifting of the sNDI group is based on conformational changes of the rigid arylsulfanyl substituents at positions 2 and 6 [see Fig. 1(a)]. This hypothesis is supported by the fact that the unsubstituted (hNDI) and pyrrolidinyl substituted (nNDI) variants did not show such switching as reported recently by Balzer *et al.* [33].

Furthermore, switched molecules appear different when scanned at positive and negative sample voltages [see Figs. 2(d)–2(f)]. Figure 2(d) shows an ordered island of
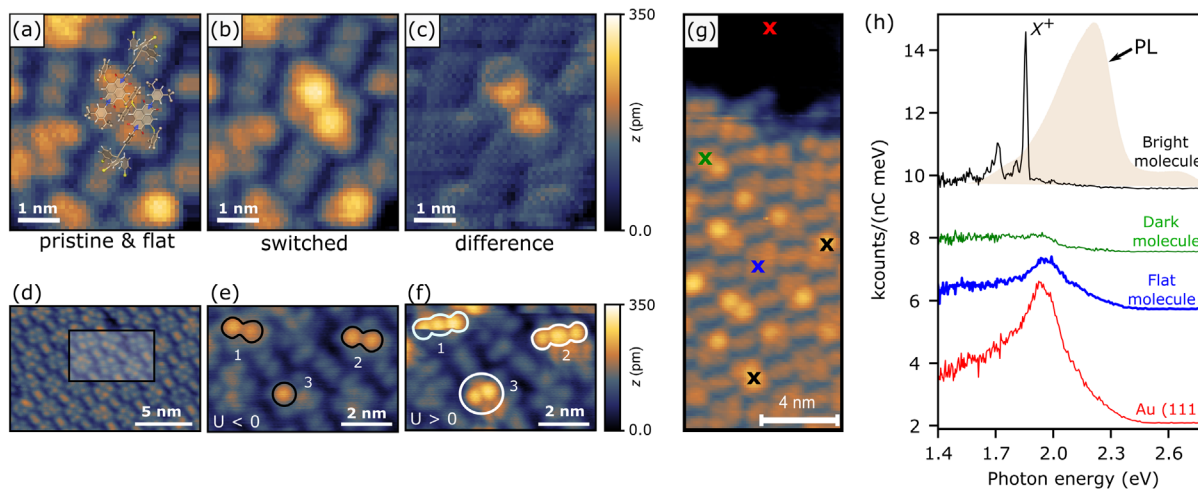
FIG. 2. Switching of Tpd-sNDI molecules. (a) Flat lying pair of Tpd-sNDI molecule with molecular structure superimposed to scale ($U = -2.5$ V, $I = 2$ pA). (b) Topography after switching both the molecules in the pair ($U = -2.6$ V, $I = 3$ pA). (c) Difference of the topographies [shown in (a) and (b)] before and after switching. (d) STM image of an ordered island ($U = 1.8$ V, $I = 2.4$ pA). (e),(f) Enlarged image of the rectangular area marked in (a) recorded at positive ($U = 2.5$ V, $I = 2.1$ pA) and negative bias ($U = -2.4$ V, $I = 2.1$ pA) voltages after switching. Molecular motifs of the switched molecules (labeled 1, 2, and 3) are marked with black and white contours. (g) STM image of an ordered island with some switched molecules showing a high feature at the position of the chromophore ($U = -2.3$ V, $I = 2$ pA). (h) Optical emission spectra recorded by placing the STM tip above different molecular motifs or Au(111). Positions of the spectra are marked with colored crosses in (b). Measurement conditions for all the spectra are $U = -2.50$ V, $I = 30$ pA, $t = 3$ s. PL spectrum is shown by yellow shaded region, recorded in dichloromethane solution with a concentration of 25 μM at ambient temperature.

Tpd-sNDI in its pristine flat state. Three molecular motifs within the masked area were then switched into a state with increased apparent height [marked 1, 2, and 3 in Figs. 2(e) and 2(f)]. Topography measurements at negative and positive sample biases show clearly different motifs. In the molecular pairs, one or both molecules can be switched which appear as one or two relatively high blobs at negative bias voltage [see Fig. 2(e)]. Moreover, the topographies at negative and positive sample biases agree with our calculations of hole and particle natural transition orbitals (see Fig. 5 herein and Fig. S3 in Supplemental Material [34]) of the molecular pairs of opposite orientation. This shows that we are able to probe the corresponding molecular frontier orbitals [black and white contours in Figs. 2(e) and 2(f)] indicating electronic decoupling of the molecules from the underlying metal substrate. Typically, this is only possible with the insertion of additional insulating layers, such as NaCl [17]. When scanning at negative bias ($U \leq -2.3$ V), most switched molecules go back to the flat configuration (see Fig. S2 in Supplemental Material [34]). Thus, there is a dependence on the polarity of the applied voltage, indicating an electric-field-driven switching mechanism. Interestingly, the molecules that do not switch back show molecule-specific EL (see the sketch in Fig. S4c [34]) as will be discussed in the following.

The EL is studied by placing the tip above different molecular motifs or above the surface of Au(111) [see Fig. 2(g)]. The EL spectrum on Au(111) shows a typical broad plasmon peak centered around 2 eV [see red

spectrum in Fig. 2(h) herein and Fig. S5a in Supplemental Material [34]]. As expected, the unswitched, i.e., flat molecules, and most of the switched molecules only act as a dielectric spacer and show no molecular EL [8,9] [see blue and green spectra in Fig. 2(h)], but a suppressed plasmon signal. The EL spectrum of some molecules, however, shows a sharp main peak (X^+) at ~1.88 eV, followed by a series of vibrational side peaks at lower energies [see black spectrum in Fig. 2(h) [35]]. We refer to them as bright molecules. The prominent vibronic side peaks (see Fig. S5b [34]) suggest evidence for the efficient decoupling of the chromophore which has not been observed in previous attempts toward tripodal self-decoupled molecules [30,32,33]. Note that the width of the peaks is limited by the instrument resolution (see Supplemental Material [34]). In the topographic channel, both switched species (dark and bright) look identical and the transition to the switched state happens at the same bias voltage. However, in flat pristine state there is a high number of slightly different variants of molecular motifs (see Fig. S4 [34]). Thus, there seem to be several possible adsorption geometries of the flat molecules from the beginning among which specific conformational geometries will emit light into the far field when switched. The difference between them, however, becomes obvious in tunneling spectroscopy, which is addressed in Fig. 3. Surprisingly, this shows that a small configuration change of the molecule can enable EL without an insulator layer.

In addition, the switched bright molecules are stable over extended periods of time (over 5–6 days) and allow
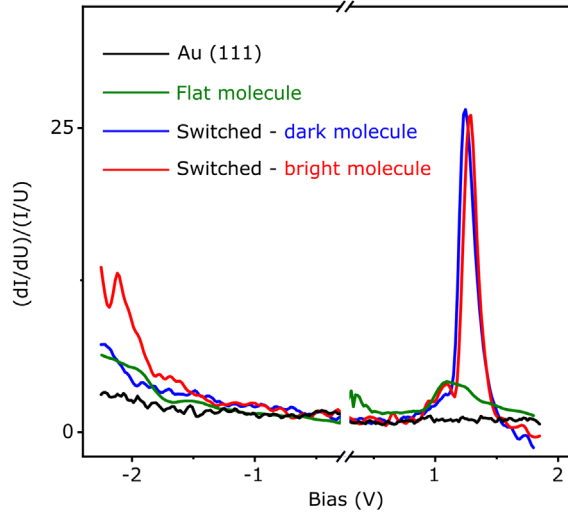
FIG. 3. Normalized dI/dU spectra measured on Au(111) (black line), on a pristine molecule (green line), on a switched dark molecule (blue line), and on a switched fluorescent molecule (red line). The low voltage, low current range has been cut out due to noise leading to a divergence of the normalized signal.

extensive EL measurements in order to explore the origin of the light emission, as will be shown later. The observed detector corrected quantum efficiency of about 10^{-5}–10^{-4} photons per electron is similar to the light emission from individual molecules deposited on insulating layers [36]. The nature of the spectra is the same for all the molecules

that show EL (see Fig. S6 [34]) and the peak positions only vary within a small energy window, which can be attributed to the Stark effect due to the presence of high electric field in the junction [37–39]. The calculated dipole moments agree with the observed Stark shifts as presented in Figs. S7 and S8 [34].

Decisive for EL is the electronic structure of the adsorbed molecule and the hybridization with the metal. To reveal the change in the electronic structure of the molecules, the normalized differential conductance $(dI/dU)/(I/U)$ was recorded on three different types of Tpd-sNDI (pristine flat molecule, switched dark molecule, and switched bright molecule; see Fig. 3). Here we normalized the differential conductance spectra to account for the large changes of the transmission probability through the vacuum at high bias voltages [40]. On the pristine flat Tpd-sNDI, a broad peak at around 1.11 V is observed (green spectrum in Fig. 3) whereas switched molecules (blue and red spectra in Fig. 3) show a much sharper peak at around 1.25 V. This indicates that the switching that we observe as a change in the apparent height at positive bias [see Fig. 2(b) herein and Fig. S3 in Supplemental Material [34]] goes along with electronic decoupling of the unoccupied orbital of the molecule, which we tentatively identify as the lowest unoccupied molecular orbital (LUMO). The FWHM extracted from a Gaussian fit changes from ~290 to ~125 meV. At negative sample bias, only the switched bright molecules show a
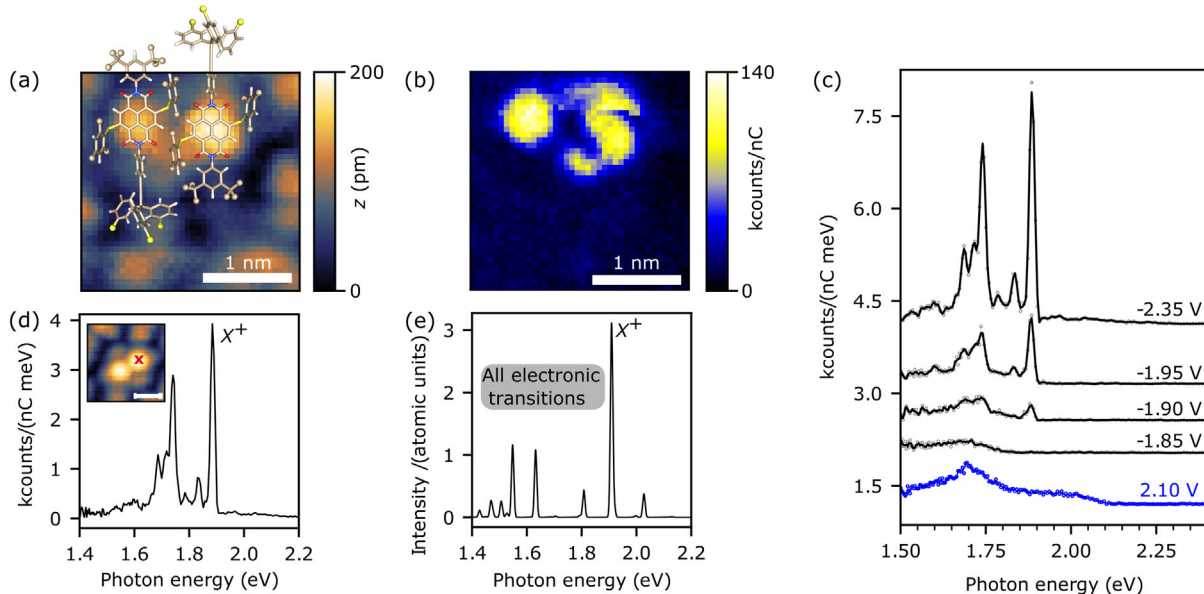

FIG. 4. Excitation of X^+ emission line. (a) Topography of switched Tpd-sNDI during the recording of the photon map shown in (b). The molecular structure is superimposed to scale. (b) Simultaneously recorded intensity of the X^+ line (grid of 40×40 points, integrated photon count in the energy range of 1.82–1.90 eV), $U = -2.3$ V, $I = 5.1$ pA, $t = 1$ s. (c) Optical emission spectra at positive (blue line) and negative (black lines) sample biases ($I = 6$ pA, $t = 60$ s). (d) Optical emission spectrum with the STM tip positioned above the switched Tpd-sNDI (see red cross in the inset topography; $U = -2.35$ V, $I = 6$ pA, $t = 60$ s). Scale bar in the inset image is 1 nm. (e) Simulated TD-CAM-B3LYP photoemission spectrum of charged pair of Tpd-sNDI showing pure electronic transitions in the indicated energy range.

peak at −2.11 V with an onset at about −1.70 V (see the red spectrum in Fig. 3), which we identify with the highest occupied molecular orbital (HOMO). These differences explain the EL behavior. For a molecule to emit light, both HOMO and LUMO need to be decoupled electronically from the metallic substrate. We find that for emission, the tunneling current needs to be injected into the orbitals of the sNDI group [see Figs. 4(a) and 4(b)]. Furthermore, bias-dependent measurements show that EL sets in as soon as the energy of the exciting electrons equals the energy of the X^+ line [see Fig. 4(c) herein and Fig. S9 in Supplemental Material [34]]. In the literature, this behavior has been explained by inelastic energy transfer mechanism [19,22] (see Fig. S10 [34]). In addition, the emission of the X^+ line is only observed at negative bias voltages [see Fig. 4(c)] and does not match the photoluminescence spectrum recorded in solution [≈2.23 eV; see Fig. 2(h)] [33] suggesting the emission from the positively charged state of the molecule [19,22,24].

To clarify the origin of the X^+ line, we performed quantum chemical calculations. The calculations for the neutral form of the Tpd-sNDI show emission lines at much higher photon energies than the X^+ line of adsorbed molecules. Furthermore, formation of pairs alone also only induces a minor shift compared to a single Tpd-sNDI molecule (see the Appendix), ruling out both possibilities. Charged monomers of Tpd-sNDI are energetically unstable, and attempts to optimize the corresponding structures ultimately lead to a decomposition into molecular fragments. However, the main line at 1.90 eV of the simulated gas phase spectrum (only electronic transitions) of the cationic form of the Tpd-sNDI pair matches well with the energy of the experimentally observed X^+ line; see Figs. 4(d) and 4(e). The calculated natural transition orbitals responsible for the emission are shown in Fig. 5, which are localized on the NDI group in agreement with the experimental observation. The hypothesis of the formation of Tpd-sNDI pairs due to the van der Waals interaction between delocalized π systems of sNDI chromophores is in good agreement with the proposed pairwise adsorption configuration [see Fig. 1(d)]. We note here that such charge-transfer excitations across two weakly bonded systems are well known [42,43]. The optimized noncovalently bonded assembly of two Tpd-sNDI molecules is shown in Fig. 7 and it supports our interpretation of the paired assembly observed experimentally.

In conclusion, our STM experiments provide evidence that it is possible to activate the EL of individual Tpd-sNDI molecules directly deposited onto a Au(111) substrate. For the first time, we were able to spatially resolve EL of molecules directly deposited on a metal surface without relying on additional insulating layers. Under the application of high positive sample bias, the adsorption geometry of sNDI group of the molecules can be switched leading to decoupling of the molecular orbitals from the conduction electrons of the metal surface so that they can be imaged with STM. Only when both HOMO and LUMO are decoupled, photon emission with quantum yields typical for single molecule EL becomes possible. Quantum chemical simulations of the gas phase spectrum reveal that the observed EL originates from the positively charged pair of the Tpd-sNDI molecule. This study opens up new pathways to achieve self-decoupled single molecule light-emitting diodes for future device applications.

Appendix: Theoretical investigation of the light-emission process.—To better understand the excitation mechanism, we performed time-dependent density function theory (TD DFT) calculations on monomeric and dimeric molecular systems. This yields qualitative insights, helping us to interpret the actual mechanism of the observed light-emission process. As outlined in the main text, the light-emission origin can best be rationalized by charged (cationic) Tpd-sNDI pairs. To elaborate on this, we calculated the excited states and corresponding natural transition orbitals (NTOs) for various molecular systems. Figure 5 shows the
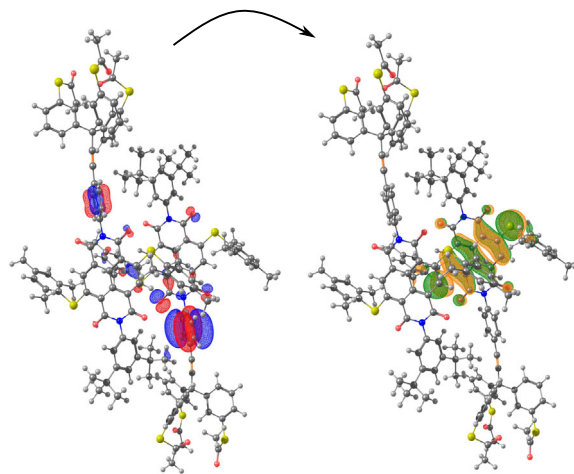

FIG. 5. Hole (left) and particle (right) natural transition orbitals (NTOs) involved in the main optical transitions of the charged Tpd-sNDI pair obtained at the TD-CAM-B3LYP/def2-TZVP (def2-SVP for H) level of theory [41].

calculated NTOs of the X^+ line for the excitation of the charged Tpd-sNDI pair formed by van der Waals interaction predicted at 1.90 eV by TD-CAM-B3LYP [44–46], being in excellent agreement with the experimentally observed main emission peak. All calculations are performed using a developed version of the TURBOMOLE package [47].

The NTO analysis of the main emission line located at 1.90 eV reveals that this is an intermolecular charge-transfer excitation, indicating the necessity of pairwise configuration in the main light-emission process. The hole NTO (Fig. 5, left-hand side) is located mainly at the edges of the chromophores, and extends to the phenyl moieties between the chromophores and the tetraphenylmethane moieties. Additionally, the hole NTO is distributed over both monomers. The particle (electron) NTO is centered on the sNDI chromophore and extends further out to the arylsulfanyl substituent (see Fig. 5, right-hand side). In contrast to the hole NTO, the particle NTO is mainly localized on a single Tpd-sNDI molecule. Charging, i.e., removing one electron, is only possible when tunneling into the particle NTO (HOMO), which is reflected in the photon map shown in Fig. 4(b). In the charged and excited dimer, the excitation process can then proceed by an electron falling from the particle to the hole NTO, emitting a photon during that process.

On the contrary, for a single neutral Tpd-sNDI molecule, no emission band below 2.00 eV could be detected that is able to cause the observed light emission at ≈ 1.90 eV. Instead, TD-CAM-B3LYP finds for the monomer a single excited state located at 2.72 eV. Therefore, no light emission can take place for a single uncharged Tpd-sNDI molecule in the investigated and accessible energy range. The NTOs reveal that the $S_0 \rightarrow S_1$ excitation resembles standard valence excitations as depicted in Fig. 6.

It is interesting to note that the particle NTO shown in Fig. 5 closely resembles the hole NTO for the monomer excitation in Fig. 6. By removing an electron, the HOMO is converted to a semioccupied molecular orbital (SOMO) like state, which is energetically lower lying and, therefore, accessible by lower-energy photons. Accordingly, photon emission connected to the HOMO $\rightarrow$ SOMO conversion will emit lower-energy photons. To finally rule out the possibility of just a neutral dimer being the source of emitted photons, we analyzed the corresponding charge-neutral system. The interaction between the monomers in the paired assembly observed in the experimental setup is mainly noncovalent, hinting at only a weak interaction between the Tpd-sNDI molecules in a neutral state.

Performing TD-CAM-B3LYP calculations on the corresponding charge-neutral Tpd-sNDI pair, shown in Fig. 7, exhibits that the peak positions of the monomers are hardly altered by the aggregation of two Tpd-sNDI molecules. Instead, two excited states with nearly the same energy are found at 2.69 and 2.73 eV. Both peaks can be attributed to the same $S_0 \rightarrow S_1$ excitation found in the monomer, being intramonomeric excitations. Accordingly, their excitations energies are virtually identical to the monomer excitation energy, too. Alterations in the molecular orbitals induced by the van der Waals interactions are therefore too shallow to account for significant shifts of energy of emitted photons, ruling out charge-neutral Tpd-sNDI pairs as the source of the emitted photons. This behavior can be expected from mainly noncovalently bonded aggregates. Even considering that the used density functional approximation, CAM-B3LYP, may exhibit a considerable blueshift for intramolecular excitations of 0.3–0.4 eV [48], neither a single Tpd-sNDI molecule nor the neutral pair alone can account for the observed occurrence of emission peaks at 1.90 eV and below. We therefore conclude that charging processes have to be taken into account to explain the observed light emission. A list of vertical excited states for
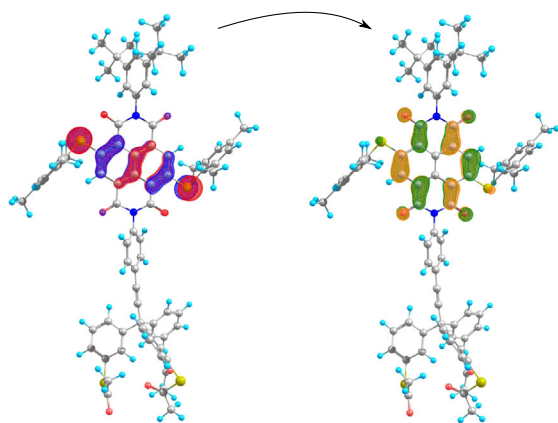

FIG. 6. Hole (left) and particle (right) NTO for the first excited state of the Tpd-sNDI monomer obtained at the TD-CAM-B3LYP/def2-TZVP (def2-SVP for H) level of theory. The excitation energy corresponding to this set of NTOs is found at 2.72 eV, ruling it out as possible source of the light emission observed in the STM experiments.
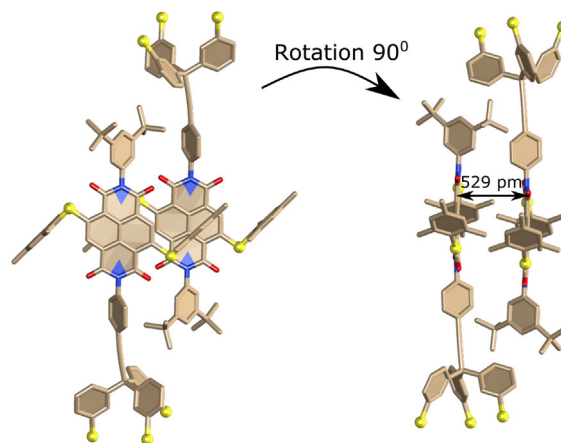

FIG. 7. Front view (left) and side view (right) of the optimized noncovalently bonded assembly of two Tpd-sNDI molecules.

the neutral monomer, the neutral paired assembly, and the cationic paired assembly is given in Table SII in Supplemental Material [34]. Vibronic effects on the excited states can unfortunately not be accessed due to the large size of the investigated systems.

---

*vibhuti.rai@kit.edu

[1] Y. Li Huang, Y. Lu, T. C. Niu, H. Huang, S. Kera, N. Ueno, A. T. S. Wee, and W. Chen, Small **8**, 1423 (2012).

[2] J. L. Zhang, J. Q. Zhong, J. D. Lin, W. P. Hu, K. Wu, G. Q. Xu, A. T. S. Wee, and W. Chen, Chem. Soc. Rev. **44**, 2998 (2015).

[3] M. Lindner, M. Valášek, M. Mayor, T. Frauhammer, W. Wulfhekel, and L. Gerhard, Angew. Chem. Int. Ed. **56**, 8290 (2017).

[4] M. Lindner, M. Valášek, M. Mayor, T. Frauhammer, W. Wulfhekel, and L. Gerhard, Angew. Chem. **129**, 8405 (2017).

[5] L. Gerhard, K. Edelmann, J. Homberg, M. Valášek, S. G. Bahoosh, M. Lukas, F. Pauly, M. Mayor, and W. Wulfhekel, Nat. Commun. **8**, 14672 (2017).

[6] L. Gerhardand M. Valášek, in *Encyclopedia of Interfacial Chemistry* (Elsevier, New York, 2018), pp. 271–280.

[7] T. Frauhammer, L. Gerhard, K. Edelmann, M. Lindner, M. Valášek, M. Mayor, and W. Wulfhekel, Phys. Chem. Chem. Phys. **23**, 4874 (2021).

[8] J. H. Coombs, J. K. Gimzewski, B. Reihl, J. K. Sass, and R. R. Schlittler, J. Microsc. **152**, 325 (1988).

[9] R. Berndt, J. K. Gimzewski, and P. Johansson, Phys. Rev. Lett. **67**, 3796 (1991).

[10] X. H. Qiu, G. V. Nazin, and W. Ho, Science **299**, 542 (2003).

[11] Z.-C. Dong, X.-L. Guo, A. S. Trifonov, P. S. Dorozhkin, K. Miki, K. Kimura, S. Yokoyama, and S. Mashiko, Phys. Rev. Lett. **92**, 086801 (2004).

[12] Z. C. Dong, X. L. Zhang, H. Y. Gao, Y. Luo, C. Zhang, L. G. Chen, R. Zhang, X. Tao, Y. Zhang, J. L. Yang, and J. G. Hou, Nat. Photonics **4**, 50 (2010).

[13] M. C. Chong, G. Reecht, H. Bulou, A. Boeglin, F. Scheurer, F. Mathevet, and G. Schull, Phys. Rev. Lett. **116**, 036802 (2016).

[14] Y. Zhang, Y. Luo, Y. Zhang, Y.-J. Yu, Y.-M. Kuang, L. Zhang, Q.-S. Meng, Y. Luo, J.-L. Yang, Z.-C. Dong, and J. G. Hou, Nature (London) **531**, 623 (2016).

[15] H. Imada, K. Miwa, M. Imai-Imada, S. Kawahara, K. Kimura, and Y. Kim, Nature (London) **538**, 364 (2016).

[16] K. Edelmann, L. Gerhard, M. Winkler, L. Wilmes, V. Rai, M. Schumann, C. Kern, M. Meyer, M. Wegener, and W. Wulfhekel, Rev. Sci. Instrum. **89**, 123107 (2018).

[17] J. Repp, G. Meyer, S. M. Stojković, A. Gourdon, and C. Joachim, Phys. Rev. Lett. **94**, 026803 (2005).

[18] H. Imada, K. Miwa, M. Imai-Imada, S. Kawahara, K. Kimura, and Y. Kim, Phys. Rev. Lett. **119**, 013901 (2017).

[19] B. Doppagne, M. C. Chong, H. Bulou, A. Boeglin, F. Scheurer, and G. Schull, Science **361**, 251 (2018).

[20] G. Chen, Y. Luo, H. Gao, J. Jiang, Y. Yu, L. Zhang, Y. Zhang, X. Li, Z. Zhang, and Z. Dong, Phys. Rev. Lett. **122**, 177401 (2019).

[21] B. Doppagne, T. Neuman, R. Soria-Martinez, L. E. P. López, H. Bulou, M. Romeo, S. Berciaud, F. Scheurer, J. Aizpurua, and G. Schull, Nat. Nanotechnol. **15**, 207 (2020).

[22] V. Rai, L. Gerhard, Q. Sun, C. Holzer, T. Repän, M. Krstić, L. Yang, M. Wegener, C. Rockstuhl, and W. Wulfhekel, Nano Lett. **20**, 7600 (2020).

[23] T.-C. Hung, B. Kiraly, J. H. Strik, A. A. Khajetoorians, and D. Wegner, Nano Lett. **21**, 5006 (2021).

[24] J. Doležal, S. Canola, P. Merino, and M. Švec, ACS Nano **15**, 7694 (2021).

[25] S. Cao, A. Rosławska, B. Doppagne, M. Romeo, M. Féron, F. Chérioux, H. Bulou, F. Scheurer, and G. Schull, Nat. Chem. **13**, 766 (2021).

[26] M. Valášek, K. Edelmann, L. Gerhard, O. Fuhr, M. Lukas, and M. Mayor, J. Org. Chem. **79**, 7342 (2014).

[27] M. Valášek, M. Lindner, and M. Mayor, Beilstein J. Nanotechnol. **7**, 374 (2016).

[28] C. W. Marquardt, S. Grunder, A. Błaszczyk, S. Dehm, F. Hennrich, H. V. Löhneysen, M. Mayor, and R. Krupke, Nat. Nanotechnol. **5**, 863 (2010).

[29] N. L. Schneider, F. Matino, G. Schull, S. Gabutti, M. Mayor, and R. Berndt, Phys. Rev. B **84**, 153403 (2011).

[30] S.-E. Zhu, Y.-M. Kuang, F. Geng, J.-Z. Zhu, C.-Z. Wang, Y.-J. Yu, Y. Luo, Y. Xiao, K.-Q. Liu, Q.-S. Meng, L. Zhang, S. Jiang, Y. Zhang, G.-W. Wang, Z.-C. Dong, and J. G. Hou, J. Am. Chem. Soc. **135**, 15794 (2013).

[31] G. Reecht, F. Scheurer, V. Speisser, Y. J. Dappe, F. Mathevet, and G. Schull, Phys. Rev. Lett. **112**, 047403 (2014).

[32] T. Ijaz, B. Yang, R. Wang, J. Zhu, A. Farrukh, G. Chen, G. Franc, Y. Zhang, A. Gourdon, and Z. Dong, Appl. Phys. Lett. **115**, 173101 (2019).

[33] N. Balzer, J. Lukášek, M. Valášek, V. Rai, Q. Sun, L. Gerhard, W. Wulfhekel, and M. Mayor, Chem. Eur. J. **27**, 12144 (2021).

[34] See Supplemental Material at http://link.aps.org/supplemental/10.1103/PhysRevLett.130.036201 for materials and methods relevant to this letter: controlled manipulation of Tpd-sNDIs, reproducibility of the emission spectra of fluorescent molecules, the influence of electric field on the emission spectra, possible mechanism behind light emission process, and calculations of possible excitation energies.

[35] B. Doppagne, M. C. Chong, E. Lorchat, S. Berciaud, M. Romeo, H. Bulou, A. Boeglin, F. Scheurer, and G. Schull, Phys. Rev. Lett. **118**, 127401 (2017).

[36] K. Kuhnke, C. Große, P. Merino, and K. Kern, Chem. Rev. **117**, 5174 (2017).

[37] J. Stark, O. Hardtke, and G. Liebert, Ann. Phys. (N.Y.) **361**, 569 (1918).

[38] H. Imada, M. Imai-Imada, K. Miwa, H. Yamane, T. Iwasa, Y. Tanaka, N. Toriumi, K. Kimura, N. Yokoshi, A. Muranaka, M. Uchiyama, T. Taketsugu, Y. K. Kato, H. Ishihara, and Y. Kim, Science **373**, 95 (2021).

[39] A. Rosławska, T. Neuman, B. Doppagne, A. G. Borisov, M. Romeo, F. Scheurer, J. Aizpurua, and G. Schull, Phys. Rev. X **12**, 011012 (2022).

[40] J. A. Stroscio, R. M. Feenstra, and A. P. Fein, Phys. Rev. Lett. **57,** 2579 (1986).

[41] F. Weigendand R. Ahlrichs, Phys. Chem. Chem. Phys. **7,** 3297 (2005).

[42] A. Dreuwand M. Head-Gordon, Chem. Rev. **105,** 4009 (2005).

[43] I. Duchemin, T. Deutsch, and X. Blase, Phys. Rev. Lett. **109,** 167801 (2012).

[44] T. Yanai, D. P. Tew, and N. C. Handy, Chem. Phys. Lett. **393,** 51 (2004).

[45] C. Bannwarth, S. Ehlert, and S. Grimme, J. Chem. Theory Comput. **15,** 1652 (2019).

[46] C. Holzer, J. Chem. Phys. **153,** 184115 (2020).

[47] S. G. Balasubramani *et al.*, J. Chem. Phys. **152,** 184107 (2020).

[48] C. Suellen, R. G. Freitas, P.-F. Loos, and D. Jacquemin, J. Chem. Theory Comput. **15,** 4581 (2019).